Lawrence Berkeley National Laboratory
Chemical Sciences

Title
Morse, Lennard-Jones, and Kratzer Potentials: A Canonical Perspective with Applications

Permalink
https://escholarship.org/uc/item/26r2n2rv

Journal
The Journal of Physical Chemistry A, 120(42)

ISSN
1089-5639

Authors
Walton, Jay R
Rivera-Rivera, Luis A
Lucchese, Robert R
et al.

Publication Date
2016-10-27

DOI
10.1021/acs.jpca.6b05371

Peer reviewed

On the Morse, Lennard-Jones, and Kratzer Potentials: A Canonical Perspective with Applications

Jay R. Walton

Department of Mathematics, Texas A&M University, College Station, Texas 77843-3368

Luis A. Rivera-Rivera[*], Robert R. Lucchese, and John W. Bevan

Department of Chemistry, Texas A&M University, College Station, Texas 77843-3255

Abstract

Canonical approaches are applied to classic Morse, Lennard-Jones, and Kratzer potentials. Using the canonical transformation generated for the Morse potential as a reference, inverse transformations allow the accurate generation of the Born-Oppenheimer potential for H_2^+ ion, neutral covalently bound H_2, van der Waals bound Ar_2, and the hydrogen bonded one dimensional dissociative coordinate in water dimer. Similar transformations are also generated using the Lennard-Jones and Kratzer potentials as references. Following application of inverse transformations, vibrational eigenvalues generated from the Born-Oppenheimer potentials give significantly improved quantitative comparison with values determined from the original accurately known potentials. In addition, an algorithmic strategy based upon a canonical transformation to dimensionless form applied to the force distribution associated to a potential is presented. The resulting canonical force distribution is employed to construct an algorithm for deriving accurate estimates for the dissociation energy, the maximum attractive force, and the internuclear separations corresponding to the maximum attractive force and the potential well.

[*] To whom correspondence should be addressed. Phone: (979) 845-8400; E-mail: rivera@chem.tamu.edu

I. Introduction

Despite advances in quantum chemistry calculations for modeling pairwise intramolecular and intermolecular interactions,[1-3] the use of empirical functional representations involving adjustable parameters for the associated model potentials still continue to play a prominent role.[4-6] Over 100 such algebraic potential forms have now been proposed[7] involving from 2 to significantly larger number of adjustable parameters. The objective has been to enhance the effectiveness of the interaction potentials involved and to increase generalized applicability and predictability of the chosen algebraic forms. Considerable effort has gone into investigating the algebraic forms that have the minimum number of variable parameters and still the most widespread applicability.[8,9] Extensive studies have also emphasized the issue of determination of universal and reduced potentials.[7,10] In no small part, the latter endeavors have had the intention of giving a fundamentally unifying approach to understanding interatomic interactions. There have also been studies to develop a simultaneous relationship among the parameters of the generalized version of the Morse, Lennard-Jones, Rydberg, and Buckingham pair potentials.[11,12] Furthermore, there is the potential for reducing computational costs associated with their application in molecular calculations for increasingly complex calculations in fields such as biochemistry and nanotechnology to name a few.[13-17]

Three specific algebraic forms for representing pairwise interactions that were among the first introduced and have had a venerated history are the Lennard-Jones[18,19] which can be regarded as a special case of the Mie potential,[20] Kratzer[21,22] and Morse[23,24] potentials. These three potentials have continued popularity for widespread applications, primarily because of limited numbers of adjustable parameters and their abilities to account for the most important inherent characteristics of the potentials they are chosen to represent. In the cases of the Kratzer

and Morse potentials, the availability of exact solutions to their Schrödinger equations have also enhanced their applicability.[25-29] Generalizations and adaptions of these potentials have also lead to more sophisticated applications.

Recently, canonical transformation approaches have also been applied to provide a different but more unifying approach to pairwise potentials.[30-33] In such studies, the concept of a pairwise canonical potential was defined for a class of molecules referred with extreme accuracy to a dimensionless function for each pairwise interatomic interaction. In constructing canonical representations of potentials, we developed an approach based upon a method for decomposing a 1-D dimensional potential curve into a finite number of canonical sections that have the same scale invariant 'shape' across a broad class of molecules. The notion of scale invariant shape utilized in this approach asserted that each designed section of the potential curve for one molecule has a unique counterpart in another molecule for which there exists an affine transformation to such a single dimensionless curve. Identification of the counterpart sections of two given dimensional potentials was found to lie with their associated force distributions. An important consequence of these studies, however, was the generation of the inverse canonical transformations necessary to provide the corresponding dimensional potentials.

We shall now demonstrate that unusual benefits can arise from applications of the Morse, Lennard-Jones, and Kratzer potentials through applications of canonical approaches.[30-33] In this work, the Born-Oppenheimer potential are accurate generated for H_2^+, H_2, Ar_2, and water dimer along the dissociative coordinate using Morse, Lennard-Jones, and Kratzer potentials as references. The generated Born-Oppenheimer potentials by canonical approaches give significantly more accurate eigenvalues than those corresponding to direct fitting for these well know potentials. Also, an algorithmic strategy based upon a canonical transformation to

3

dimensionless form applied to the force distribution associated to a potential is presented. Ramifications associated with utilization of these canonical approaches to the specific potentials considered and other algebraic potentials will also be discussed.

II. Methods

In ref 33, a notion of *transformation to canonical form* for two one-dimensional potentials was introduced and studied for a class of diatomic molecules within the Born-Oppenheimer approximation. This transformation involves decomposing the two potential curves into a finite number of sections for which there exist affine transformations of corresponding sections to the same dimensionless curve. The identification of the corresponding sections of the two potential curves is based upon their associated *Feynman Force* distributions.[34] Appealing to the inverses of these affine transformations to canonical form, one then can construct a piecewise affine representation of one of the potentials in terms of the other. This procedure was expanded to a class of diatomic molecules (more than two) by declaring one of their potentials to be reference and constructing piecewise affine representations of all other potential curves in the chosen class in terms of the reference molecule. In ref 33, H_2^+ was chosen as reference with the remaining molecules within the class considered being HeH^+, LiH and H_2 due to the availability of their extremely accurate potentials within the Born-Oppenheimer approximation.

The transformation to canonical form and its associated piecewise affine transformation between two different potential curves exploited in ref 33, is distinctly different from the traditional process of constructing approximations to potential curves within a specified family of functions depending upon a finite number of free parameters.[7] In the present work, it is shown how the two points of view can be perceived in stark contrast by applying the above

transformation to canonical form to three of the simplest classical algebraic potential forms: the Kratzer potential,[21,22] the Morse potential,[23,24] and both a classic[18,19] and a generalized Lennard-Jones potential that are defined as follows. In the following definitions, $D_e = E(R_e)$ denotes the well depth (dissociation energy for a diatomic molecule) for the potential, R_e denotes the equilibrium separation distance of the nuclei for a diatomic molecule, and R_{am} denotes the separation distance of the nuclei at which the attractive (Feynman) force has maximum magnitude, *i.e.* the inflection point of $E(R)$.

The Kratzer potential is a simple, two-parameter model. The two parameters are customarily chosen to be D_e and R_e in which case the potential takes the form

$$E_K(R) := D_e\left(\left(\frac{R_e}{R}\right)^2 - 2\left(\frac{R_e}{R}\right)\right). \tag{1}$$

The Morse potential is a three-parameter model. Two of the parameters are customarily chosen to be D_e and R_e in which case the potential takes the form

$$E_M(R) := D_e\left(\left(1 - \exp\left(-a\left(R - R_e\right)\right)\right)^2 - 1\right). \tag{2}$$

Many strategies have been used in the literature for determining a value for the free parameter a in eq 2. From the perspective of the transformation to canonical form utilized in ref 33, it is natural to choose a in eq 2 so that the potential form interpolates the accurate potential at $R = R_{am}$. In that case, one can show that eq 2 takes the form

$$E_M(R) := D_e\left(\left(1 - \left(\frac{1}{2}\right)^{\left(\left(R/R_e\right)-1\right)/\left(\left(R_{am}/R_e\right)-1\right)}\right)^2 - 1\right). \tag{3}$$

A generalized Lennard-Jones potential is defined here to be a four-parameter model of the form

$$E_{LJ}(R;n,\alpha) := \frac{D_e}{\alpha-1}\left(\left(\frac{R_e}{R}\right)^{\alpha n} - \alpha\left(\frac{R_e}{R}\right)^n\right). \tag{4}$$

It is seen immediately that the Kratzer potential, eq 1, is a special case of the generalized Lennard-Jones potential in eq 4. Indeed, one has $E_K(R) = E_{LJ}(R;1,2)$. Also, the classical (6,12)-Lennard-Jones potential has $n=6$ and $\alpha=2$.

A. The Morse Potential as Reference

In ref 33, the potential for H_2^+ was chosen as reference for the class of diatomic molecules considered. The inverse canonical transformation was then used to construct approximations to the potentials for all molecules in the considered class as piecewise affine scalings of the reference potential. The same procedure is employed here except that the Morse potential[23,24] is chosen as reference and the considered class contains two of the four molecules examined, namely H_2 (ref 35) and H_2^+ (ref 36), plus Ar_2 (ref 37) and the water dimer[38] complex. The derivation of the construction is given in detail in ref 33; only the results required for the key formulas are included here.

1. Identification of Canonical Sections of Potential Curves: The Associated Feynman Force

Let $E(R)$ be the potential for a molecule in the considered class and $F(R) := -E'(R)$ be its associated (Feynman) force. Let R_e and R_{am} be as defined above, or equivalently, the unique R–values satisfying $F(R_e) = F'(R_{am}) = 0$. Next define $F_m := |F(R_{am})|$, that is, F_m is the magnitude of the maximum attractive value of the (Feynman) force. Then define the (diadic) sequence

$$\ldots < R_{rj} < R_{r(j-1)} < \ldots < R_{r1} < R_{rm} < R_e < R_{am} < R_{a1} < \ldots < R_{aj} < \ldots \tag{5}$$

by the following formulas: for $j = 0, 1, \ldots$,

$$F(R_{rj}) = F_m 2^j \tag{6}$$

$$F(R_{aj}) = -F_m / 2^j.$$ (7)

It is noted that in this notation $R_{rm} = R_{r0}$ and $R_{am} = R_{a0}$.

Similarly, for the Morse potential eq 2, let $F_M(R) := -E'_M(R)$ denote its associated (Feynman) force and construct its (diadic) sequence of separation distances corresponding to eq 5

$$\ldots < R_{M,rj} < R_{M,r(j-1)} < \ldots < R_{M,r1} < R_{M,rm} < R_{M,e} < R_{M,am} < R_{M,a1} < \ldots < R_{M,aj} < \ldots$$ (8)

with

$$F_M(R_{M,rj}) = F_{M,m} 2^j$$ (9)

$$F_M(R_{M,aj}) = -F_{M,m} / 2^j.$$ (10)

The R_{rj}, R_{aj}, $R_{M,rj}$, and $R_{M,aj}$ values determine the sections of the potential curves $E(R)$ and $E_M(R)$ for which there exists an affine transformation of each to a common dimensionless canonical form. For the application considered here, the following R–values are used to derive the piecewise affine transformations given below: R_{r5}, R_{r3}, R_{r1}, R_{rm}, R_e, R_{am}, R_{a1}, R_{a3}, R_{a5}. Thus, the sections of the Morse potential curve defined by $R_{M,r5} < R < R_{M,r3}$ and of a target molecule by $R_{r5} < R < R_{r3}$ are canonical, etc. It is noted that by definition $R_{M,e} = R_e$ and $D_{M,e} = D_e$. Appealing to the inverse affine canonical transformation derived in ref 33 one constructs the following piecewise affine representation $\tilde{E}_M(R)$ of $E(R)$ in terms of $E_M(R)$.

$$
\tilde{E}_{\mathrm{M}}(R)=\begin{cases}
E(R_{\mathrm{r3}})+\left(\dfrac{E(R_{\mathrm{r5}})-E(R_{\mathrm{r3}})}{E_{\mathrm{M}}(R_{\mathrm{M,r5}})-E_{\mathrm{M}}(R_{\mathrm{M,r3}})}\right)\left(E_{\mathrm{M}}\left(R_{\mathrm{M,r3}}+\dfrac{(R_{\mathrm{M,r5}}-R_{\mathrm{M,r3}})(R-R_{\mathrm{r3}})}{(R_{\mathrm{r5}}-R_{\mathrm{r3}})}\right)-E_{\mathrm{M}}(R_{\mathrm{M,r3}})\right), & R_{\mathrm{r5}}<R<R_{\mathrm{r3}}\\[3ex]
E(R_{\mathrm{r1}})+\left(\dfrac{E(R_{\mathrm{r3}})-E(R_{\mathrm{r1}})}{E_{\mathrm{M}}(R_{\mathrm{M,r3}})-E_{\mathrm{M}}(R_{\mathrm{M,r1}})}\right)\left(E_{\mathrm{M}}\left(R_{\mathrm{M,r1}}+\dfrac{(R_{\mathrm{M,r3}}-R_{\mathrm{M,r1}})(R-R_{\mathrm{r1}})}{(R_{\mathrm{r3}}-R_{\mathrm{r1}})}\right)-E_{\mathrm{M}}(R_{\mathrm{M,r1}})\right), & R_{\mathrm{r3}}<R<R_{\mathrm{r1}}\\[3ex]
E(R_{\mathrm{rm}})+\left(\dfrac{E(R_{\mathrm{r1}})-E(R_{\mathrm{rm}})}{E_{\mathrm{M}}(R_{\mathrm{M,r1}})-E_{\mathrm{M}}(R_{\mathrm{M,rm}})}\right)\left(E_{\mathrm{M}}\left(R_{\mathrm{M,rm}}+\dfrac{(R_{\mathrm{M,r1}}-R_{\mathrm{M,rm}})(R-R_{\mathrm{rm}})}{(R_{\mathrm{r1}}-R_{\mathrm{rm}})}\right)-E_{\mathrm{M}}(R_{\mathrm{M,rm}})\right), & R_{\mathrm{r1}}<R<R_{\mathrm{rm}}\\[3ex]
-D_{\mathrm{e}}+\left(\dfrac{E(R_{\mathrm{rm}})+D_{\mathrm{e}}}{E_{\mathrm{M}}(R_{\mathrm{M,rm}})+D_{\mathrm{e}}}\right)\left(E_{\mathrm{M}}\left(R_{\mathrm{e}}+\dfrac{(R_{\mathrm{M,rm}}-R_{\mathrm{e}})(R-R_{\mathrm{e}})}{(R_{\mathrm{rm}}-R_{\mathrm{e}})}\right)+D_{\mathrm{e}}\right), & R_{\mathrm{rm}}<R<R_{\mathrm{e}}\\[3ex]
-D_{\mathrm{e}}+\left(\dfrac{E(R_{\mathrm{am}})+D_{\mathrm{e}}}{E_{\mathrm{M}}(R_{\mathrm{M,am}})+D_{\mathrm{e}}}\right)\left(E_{\mathrm{M}}\left(R_{\mathrm{e}}+\dfrac{(R_{\mathrm{M,am}}-R_{\mathrm{e}})(R-R_{\mathrm{e}})}{(R_{\mathrm{am}}-R_{\mathrm{e}})}\right)+D_{\mathrm{e}}\right), & R_{\mathrm{e}}<R<R_{\mathrm{am}}\\[3ex]
E(R_{\mathrm{am}})+\left(\dfrac{E(R_{\mathrm{a1}})-E(R_{\mathrm{am}})}{E_{\mathrm{M}}(R_{\mathrm{M,a1}})-E_{\mathrm{M}}(R_{\mathrm{M,am}})}\right)\left(E_{\mathrm{M}}\left(R_{\mathrm{M,am}}+\dfrac{(R_{\mathrm{M,a1}}-R_{\mathrm{M,am}})(R-R_{\mathrm{am}})}{(R_{\mathrm{a1}}-R_{\mathrm{am}})}\right)-E_{\mathrm{M}}(R_{\mathrm{M,am}})\right), & R_{\mathrm{am}}<R<R_{\mathrm{a1}}\\[3ex]
E(R_{\mathrm{a1}})+\left(\dfrac{E(R_{\mathrm{a3}})-E(R_{\mathrm{a1}})}{E_{\mathrm{M}}(R_{\mathrm{M,a3}})-E_{\mathrm{M}}(R_{\mathrm{M,a1}})}\right)\left(E_{\mathrm{M}}\left(R_{\mathrm{M,a1}}+\dfrac{(R_{\mathrm{M,a3}}-R_{\mathrm{M,a1}})(R-R_{\mathrm{a1}})}{(R_{\mathrm{a3}}-R_{\mathrm{a1}})}\right)-E_{\mathrm{M}}(R_{\mathrm{M,a1}})\right), & R_{\mathrm{a1}}<R<R_{\mathrm{a3}}\\[3ex]
E(R_{\mathrm{a3}})+\left(\dfrac{E(R_{\mathrm{a5}})-E(R_{\mathrm{a3}})}{E_{\mathrm{M}}(R_{\mathrm{M,a5}})-E_{\mathrm{M}}(R_{\mathrm{M,a3}})}\right)\left(E_{\mathrm{M}}\left(R_{\mathrm{M,a3}}+\dfrac{(R_{\mathrm{M,a5}}-R_{\mathrm{M,a3}})(R-R_{\mathrm{a3}})}{(R_{\mathrm{a5}}-R_{\mathrm{a3}})}\right)-E_{\mathrm{M}}(R_{\mathrm{M,a3}})\right), & R_{\mathrm{a3}}<R<R_{\mathrm{a5}}
\end{cases}
$$

$$(11)$$

Analogous expressions are readily constructed for the Lennard-Jones and Kratzer potentials as references. In the following section, the representation in eq 11, and its Lennard-Jones and Kratzer versions, are applied to the three diatomic molecules H_2, H_2^+, Ar_2 along with the water dimer complex. For water dimers, the pairwise interaction is specified with respect to the radial dissociative coordinate of the dimer, while frozen all other coordinates to that of the equilibrium geometry of the dimer.

III. Results and Discussion

Figures 1-3 give a graphical summary of the key distinction between the classical and canonical approaches to utilizing the Morse, Lennard-Jones, and Kratzer potentials to

approximate the 1-dimensional potentials for the diatomic molecules H_2, H_2^+, and Ar_2, and the water dimer complex. In particular, Figure 1 gives graphical results for the Morse potential. The solid line is the accurate potential curve while the dashed line is the *classical* Morse approximation $E_M(R)$ as discussed previously. The open red circles correspond to the *canonical* Morse approximation $\tilde{E}_M(R)$ as encapsulated in the representation eq 11.

The solid red circles on the abscissa denote the R_j values for $E(R)$ used in eq 11, while the blue stars denote the corresponding R_{Mj} values for $E_M(R)$ used in eq 11. The solid red circles on the solid black curve illustrate the segmented decomposition of the accurate potential curve $E(R)$, while the blue stars on the dashed curve give the corresponding curve segments on the classical Morse approximation $E_M(R)$. Thus, a segment on the accurate potential curve $E(R)$ defined by two successive solid red circles and its counterpart on the dashed curve between the corresponding successive blue stars have *canonical shapes* in the sense that each has an affine mapping to a common dimensionless curve. What the construction eq 11 does is map each segment on the dashed curve between two successive blue stars to its counterpart on the solid curve between the corresponding solid red circles. It is important to emphasize that the affine scalings comprising eq 11 map the blue star segment endpoints to the solid red circle endpoints; the open red circles illustrate the sense in which the two segments do indeed have the same shape. The first line of Table 1 gives the relative errors between the accurate potential curves $E(R)$ (solid black curves in Figure 1) and the canonical Morse potential approximations $\tilde{E}_M(R)$ (open red circles in Figure 1). It should be remarked that the relative error between the accurate potential $E(R)$ and the classical Morse approximation $E_M(R)$ is more than two orders of magnitude larger than for the canonical Morse approximation $\tilde{E}_M(R)$. The notion of relative error used in Table 1 is defined by

$$\text{Relative Error} = \frac{\int_{R_{r5}}^{R_{a5}} \left| E(R) - \tilde{E}(R) \right| dR}{\int_{R_{r5}}^{R_{a5}} \left| E(R) \right| dR}. \tag{12}$$

Figures 2 and 3 illustrate the corresponding results for the Lennard-Jones and Kratzer potentials. It should be noted that the difference between the classical and canonical approaches to approximating a potential is illustrated rather dramatically by the Kratzer potential applied to Ar_2 and the water dimer complex. In particular, Table 2 shows that for Ar_2, $R_{a3} = 5.91$ Å and $R_{a5} = 7.1$ Å, while for the corresponding classical Kratzer approximation, $E_K(R)$, $R_{K,a3} = 25.52$ Å and $R_{K,a5} = 53.3$ Å, yet the segment of the accurate Ar_2 curve (solid curve in Figure 3) between $R_{a3} < R < R_{a5}$ and the corresponding classical Kratzer approximation segment (dashed curve in Figure 3) between $R_{K,a3} < R < R_{K,a5}$ have the same canonical shape. More specifically, there is a simple affine transformation that takes the latter curve onto the former with relative error less than 0.001.

It is important to emphasize that these results imply that for a given molecule, the canonical Morse, Lennard-Jones, and Kratzer approximations to the accurate potential are *equivalent* to high order of accuracy. Furthermore, each of the classical Morse, Lennard-Jones, and Kratzer potentials can be used in the construction eq 11 to provide canonical approximations of the other two to high order of accuracy.

As a test of the Morse canonical approximation, we calculated all vibrational eigenvalues for the accurate, the canonical Morse approximation, and the classical Morse approximation potentials for H_2, H_2^+, Ar_2, and water dimer complex. The corresponding eigenvalues are given in Tables 3-5, and they were calculated using a modify Numerov-Cooley approach.[39] As apparent, the canonical Morse approximation potential predicts all vibrational eigenvalues in

dramatically closer agreement with the accurate potential than with the classical Morse approximation potential. It is noted that a better accuracy in the Morse canonical approximation potential can be achieved by using more R_{rj} and R_{aj} values.[33]

There have been extensive investigations of simultaneous relationships among parameters of empirical interatomic potential functions to investigate the similarities and differences between such potentials.[11,12] From a practical perspective, this information is helpful in converting parametric data from one function to another, particularly when such functions are utilized in software packages. Lennard-Jones potentials are used extensively for describing paired potentials of van der Waals interactions in software packages such as CHARM[40] and AMBER[41] whereas the Morse potential is frequently adapted in computational chemistry for CVFF[42] and UFF[43] software packages. The currently developed approach should find useful applications in such software packages while generalizing and facilitating application of a wide range of empirical functional forms, while de-emphasizing the significance of the adjustable parameters.

IV. Applications

The results discussed above demonstrate that the potential curves for the considered molecules (H_2, H_2^+, Ar_2 and water dimer) and the potential curves associated with the classical Morse, Lennard-Jones, and Kratzer potentials all have the same canonical shape. Moreover, this notion of canonical shape can be exploited to construct through elementary formulas approximations to the potential curves for the considered molecules from any one of the classical Morse, Lennard-Jones, and Kratzer potential curves to high accuracy. These results give rise to two obvious questions. *i*) Can this idea be exploited to devise a practical tool for constructing force and potential curves? *ii*) How essential is it to know the exact R-values in eq 11 and the

accurate potential values at those *R*-values? The answer to the first question is yes as will be shown below. The answer to the second question is that knowing the *R*-values in eqs 5 and 11 and the accurate potential values at those *R*-values was sufficient to demonstrate the asserted canonical shape properties and construct highly accurate approximations to the accurate potentials for the considered molecules from the classical Morse, Lennard-Jones, and Kratzer potential curves, but is not necessary. Below we give a stepwise algorithm for generalizing the constructions of the first part of this paper that does not require knowledge of the precise *R*-values in eq 5 or a subsequence thereof. The first step in the algorithm makes use of the canonical shape property to approximate to high accuracy the four key quantities: R_e, D_e, R_{am}, and F_m.

A. Stepwise Algorithm

Step (*i*)

As argued in ref 32, the canonical shape property for *force* is more fundamental than the canonical shape property of its associated potential. In particular, exploiting the canonical shape property of force to construct accurate approximations to the force curve associated to a molecule immediately gives (through integration) an accurate approximation to the associated potential but the reverse is, in general, not the case; that is, a highly accurate approximation to a potential curve, when differentiated, can yield an approximation to the force with arbitrarily large error.

The property of canonical force curve shape can be used to give highly accurate approximations of R_e, D_e, R_{am}, and F_m for a given molecule from the force curve corresponding to any one of the classical Morse, Lennard-Jones, and Kratzer potentials. The construction proceeds as follows in which we choose the classical (6,12)-Lennard-Jones potential as reference

12

and any generic target molecule. The procedure is then applied to each of the four molecules considered previously.

1. Canonical Force Curve

Let $E_{LJ}(R)$ denote the classical (6,12)-Lennard-Jones potential with $F_{LJ}(R) = -E'_{LJ}(R)$ being its associated force. Similarly, let $E(R)$ denote the target potential with associated force $F(R) = -E'(R)$. Let $R_{LJ,e}$ and R_e denote the R-location of the potential well for the Lennard-Jones and target potentials, respectively. Analogously, $R_{LJ,am}$ and R_{am} denote the R-locations where the attractive force is maximum (inflection point) and let $F_{LJ,m}$ and F_m denote the magnitude of the maximum attractive force. The canonical force curves corresponding to the sections of these force curves between the well bottom and the inflection point are defined by

$$CF_{LJ,eam}(x) = F_{LJ}(xR_{LJ,am} + (1-x)R_{LJ,e}) / F_{LJ,m} \tag{13}$$

$$CF_{eam}(x) = F(xR_{am} + (1-x)R_e) / F_m. \tag{14}$$

From eqs 13 and 14 an approximation for the force curve $F(R)$ over $R_e \leq R \leq R_{am}$ in terms the canonical force eq 13 for the Lennard-Jones force can be constructed through

$$\tilde{F}_{eam}(R) = F_m CF_{LJ,eam}\left(\frac{R - R_e}{R_{am} - R_e}\right). \tag{15}$$

This is the *forward* canonical approximation of the target force $F(R)$ by the reference force $F_{LJ}(R)$ via the dimensionless canonical shape functions. The idea now is to treat R_e, R_{am}, and F_m in eq 15 as unknowns. To find these values, one selects three R-values $\{R_0 < R_1 < R_2\}$ on the open interval $R_e < R < R_{am}$. Having a rough idea of the accurate values R_e and R_{am} could gives to a better estimate of the initial guess values. Next, assuming that good approximate values for the accurate force $F(R_j)$, $j = 0,1,2$ have been obtained (from *ab initio* calculation or experimental data, for example), a three-by-three system of algebraic equations can be formulate

$$F(R_j) = F_m CF_{\text{LJ,eam}}\left(\frac{R_j - R_e}{R_{am} - R_e}\right), \quad j = 0,1,2 \tag{16}$$

and solves for approximations of R_e, R_{am}, and F_m. The system in eq 16 is readily solved using standard numerical software. Table 6 shows the results of applying this algorithm to each of the four target molecules H_2, H_2^+, Ar_2, and water dimer obtaining estimates for R_e, R_{am}, and F_m.

To approximate D_e the dimensionless canonical potential curves are use

$$CE_{\text{LJ,eam}}(x) = \frac{E_{\text{LJ}}(xR_{\text{LJ,am}} + (1-x)R_{\text{LJ,e}}) + D_{\text{LJ,e}}}{E_{\text{LJ}}(R_{\text{LJ,am}}) + D_{\text{LJ,e}}} \tag{17}$$

$$CE_{\text{eam}}(x) = \frac{E(xR_{am} + (1-x)R_e) + D_e}{E(R_{am}) + D_e}, \tag{18}$$

and the associated approximation of the accurate potential $E(R)$ by the canonical transformation of the Lennard-Jones potential $CE_{\text{LJ,eam}}(x)$ (eq 17) is given by

$$\tilde{E}_{\text{eam}}(R) = -D_e + (E(R_{am}) + D_e)CE_{\text{LJ,eam}}\left(\frac{R - R_e}{R_{am} - R_e}\right). \tag{19}$$

In eq 19 assumes that a good approximation to the accurate $E(R_{am})$ value is know from experimental data or *ab initio* calculation. As before, D_e is treats as unknown parameter in eq 19. Assuming that a good approximation to the accurate value $E(R_0)$ is know, an approximation to D_e can be obtained by solving the algebraic equation

$$E(R_0) = -D_e + (E(R_{am}) + D_e)CE_{\text{LJ,eam}}\left(\frac{R_0 - R_e}{R_{am} - R_e}\right) \tag{20}$$

for the unknown value D_e. Eqs 19 and 20 used the approximate vales of R_e and R_{am}. In Table 6 this process produces an approximation to the accurate value of D_e for each of the four target molecules.

Step (ii)

The second step of the algorithm involves constructing a piecewise approximation to the force curve for the target molecule from the canonical force curves of the reference potential. The algorithm makes use of the approximate values of R_e, R_{am}, and F_m constructed in Step (i) and considers the repulsive ($0 < R < R_e$) and attractive ($R_e < R$) sides of the force curve separately.

2. Repulsive Side

First an arbitrary R-value $R_{rm} < R_e$ for the target molecule is chosen. This defines a section of the target force curve defined for $R_{rm} < R < R_e$. The issue at hand is how to choose the corresponding section of the reference Lennard-Jones force curve $F_{LJ}(R)$, $R_{LJ,rm} < R < R_e$ with the same canonical shape. Assuming that a good approximation (from *ab initio* calculations or spectroscopic data, for example) for the force $F(R_{rm})$ is know, the reference point $R_{LJ,rm}$ is chosen as the solution to the algebraic equation

$$\frac{F_{LJ}(R_{LJ,rm})}{F_{LJ,m}} = \frac{F(R_{rm})}{F_m} \tag{21}$$

where the approximated value of F_m given in Table 6 is used. The target force $F(R)$ can then be approximated on $R_{rm} \leq R \leq R_e$ by

$$\tilde{F}_{rme}(R) = F_m CF_{LJ,rme}\left(\frac{R - R_e}{R_{rm} - R_e}\right) \tag{22}$$

where the approximated value of F_m and R_e given in Table 6 are used and the dimensionless canonical force function $CF_{LJ,rme}(x)$, $0 \leq x \leq 1$ is defined by

$$CF_{LJ,rme}(x) = \frac{F_{LJ}(xR_{LJ,e} + (1-x)R_{LJ,rm}) - F_{LJ}(R_{LJ,rm})}{F_{LJ}(R_{LJ,e}) - F_{LJ}(R_{LJ,rm})}. \tag{23}$$

An obvious question is how arbitrary is the choice of R_{rm}? The issue is one of desired accuracy in the approximation. The discussions of canonical transformations in the first part of

15

the paper and in ref 33 suggest that good accuracy will be achieved provided $|F(R_{\mathrm{rm}})| \leq F_{\mathrm{m}}$, where F_{m} is given in Table 6.

Similarly, a second R-value $R_{\mathrm{r1}} < R_{\mathrm{rm}}$ is chosen with a good approximation of the force $F(R_{\mathrm{r1}})$ for the target force curve and then calculates the corresponding R-value $R_{\mathrm{LJ,r1}} < R_{\mathrm{LJ,rm}}$ for the reference Lennard-Jones force curve to be the solution of the algebraic equation

$$\frac{F_{\mathrm{LJ}}(R_{\mathrm{LJ,r1}})}{F_{\mathrm{LJ,m}}} = \frac{F(R_{\mathrm{r1}})}{F_{\mathrm{m}}}. \tag{24}$$

The target force $F(R)$ can be approximated on $R_{\mathrm{r1}} \leq R \leq R_{\mathrm{rm}}$ by

$$\tilde{F}_{\mathrm{r1rm}}(R) = F(R_{\mathrm{rm}}) + (F(R_{\mathrm{r1}}) - F(R_{\mathrm{rm}}))CF_{\mathrm{LJ,r1rm}}\left(\frac{R - R_{\mathrm{rm}}}{R_{\mathrm{r1}} - R_{\mathrm{rm}}}\right) \tag{25}$$

where the dimensionless canonical force function $CF_{\mathrm{LJ,r1rm}}(x)$, $0 \leq x \leq 1$ is defined by

$$CF_{\mathrm{LJ,r1rm}}(x) = \frac{F_{\mathrm{LJ}}(xR_{\mathrm{LJ,rm}} + (1-x)R_{\mathrm{LJ,r1}}) - F_{\mathrm{LJ}}(R_{\mathrm{LJ,r1}})}{F_{\mathrm{LJ}}(R_{\mathrm{LJ,rm}}) - F_{\mathrm{LJ}}(R_{\mathrm{LJ,r1}})}. \tag{26}$$

Again the question of how arbitrary the choice of R_{r1} is arises. The results in ref 33 suggest that a conservative restriction is that $|F(R_{\mathrm{LJ,r1}})| \leq 2.0F_{\mathrm{m}}$.

The algorithm proceeds inductively by choosing as many R-values as desired depending upon how much of the repulsive wall need to be cover. For illustrative purposes, only five values $R_{\mathrm{r4}} < \ldots < R_{\mathrm{rm}}$ were selected for each of the target molecules given in Table 7. As seen in Table 7, all of the relative errors in the force approximations over $R_{\mathrm{r4}} < R < R_{\mathrm{e}}$ are less than 0.005. A measure of how far up the repulsive wall the approximations go is given by the dimensionless ratio $|F(R_{\mathrm{r4}})|/F_{\mathrm{m}}$. For the four test molecules H_2, H_2^+, Ar_2, and water dimer, this ratio takes the values 10.49, 13.42, 43.3 and 85.78, respectively.

3. Attractive Side

For the attractive side, the modified strategy for selecting R-values introduced in ref 44 is employed to enhance accuracy. This strategy is based upon the fact that "shape" information about a function is encoded in its derivative. Thus, we use $F'(R)$ and $F'_{\mathrm{LJ}}(R)$ to select R-values for both the target and reference force curves $F(R)$ and $F_{\mathrm{LJ}}(R)$ for $R > R_{\mathrm{e}}$. To that end, we must find approximations to R_{fm} and F_{fm}, where F_{fm} is the maximum value of $|F'(R)|$ for $R > R_{\mathrm{am}}$ and $R_{\mathrm{fm}} > R_{\mathrm{am}}$ satisfies $|F'(R_{\mathrm{fm}})| = F_{\mathrm{fm}}$. An algorithm for approximating R_{fm} and F_{fm} is readily constructed in a similar manner to the one used above to approximate R_{am}, R_{e}, and F_{m}. Specifically, two R-values $R_{\mathrm{am}} < R_3 < R_4$ are selected and approximations to $F'(R_3)$ and $F'(R_4)$ are obtained. Next, approximations to R_{fm} and F_{fm} are obtained by solving the algebraic system

$$F'(R_j) = F_{\mathrm{fm}} CF_{\mathrm{LJ,fm}}\left(\frac{R_j - R_{\mathrm{am}}}{R_{\mathrm{fm}} - R_{\mathrm{am}}}\right), \quad j = 3,4 \tag{27}$$

for R_{fm} and F_{fm} where $CF_{\mathrm{LJ,fm}}(x)$, $0 \leq x \leq 1$ is the dimensionless canonical function

$$CF_{\mathrm{LJ,fm}}(x) = \frac{F'_{\mathrm{LJ}}(xR_{\mathrm{LJ,fm}} + (1-x)R_{\mathrm{LJ,am}})}{F_{\mathrm{LJ,fm}}}. \tag{28}$$

In eq 28, $R_{\mathrm{LJ,fm}}$ and $F_{\mathrm{LJ,fm}}$ are defined by

$$F_{\mathrm{LJ,fm}} = |F'_{\mathrm{LJ}}(R_{\mathrm{LJ,fm}})| = \max |F'_{\mathrm{LJ}}(R)|, \quad R > R_{\mathrm{am}}. \tag{29}$$

Since $F_{\mathrm{LJ}}(R)$ is given by a simple algebraic formula, $F_{\mathrm{LJ,fm}}$ and $R_{\mathrm{LJ,fm}}$ are easily calculated to very high accuracy. Table 6 gives the approximate values for F_{fm} and R_{fm} obtained from solving the system in eq 27 for each of the four considered target molecules, and the values for R_3 and R_4 used to that end.

The approximation to $F(R)$ for $R_e < R$ for a target molecule in terms of the reference Lennard-Jones force curve is now constructed as follows. For $R_e \leq R \leq R_{am}$, the approximation is given by eq 15. For $R_{am} \leq R \leq R_{fm}$, the approximation to $F(R)$ takes the form

$$\tilde{F}_{amfm}(R) = F_m + (F_{fm} - F_m)CF_{LJ,amfm}\left(\frac{R - R_{am}}{R_{fm} - R_{am}}\right) \tag{30}$$

where the dimensionless canonical force $CF_{LJ,amfm}(x)$, $0 \leq x \leq 1$ is defined by

$$CF_{LJ,amfm}(x) = \frac{F_{LJ}(xR_{LJ,fm} + (1-x)R_{LJ,am}) - F_{LJ}(R_{LJ,am})}{F_{LJ}(R_{LJ,fm}) - F_{LJ}(R_{LJ,am})}. \tag{31}$$

To approximate $F(R)$ for $R > R_{fm}$, first an arbitrary $R_{a2} > R_{fm}$ is chosen for the target molecule and an approximate value for $F'(R_{a2})$ (from *ab initio* calculation or experimental data, for example) is obtained. The corresponding R-value $R_{LJ,a2}$ for the reference force curve is the unique solution to the algebraic equation

$$\frac{F'_{LJ}(R_{LJ,a2})}{F_{LJ,fm}} = \frac{F'(R_{a2})}{F_{fm}}. \tag{32}$$

The approximation to $F(R)$ for $R_{fm} \leq R \leq R_{a2}$ then takes the form

$$\tilde{F}_{fma2}(R) = F(R_{fm}) + (F(R_{a2}) - F(R_{fm}))CF_{LJ,fma2}\left(\frac{R - R_{fm}}{R_{a2} - R_{fm}}\right) \tag{33}$$

where the dimensionless canonical force $CF_{LJ,fma2}(x)$, $0 \leq x \leq 1$, for the reference Lennard-Jones force curve is defined by

$$CF_{LJ,fma2}(x) = \frac{F_{LJ}(xR_{LJ,a2} + (1-x)R_{LJ,fm}) - F_{LJ}(R_{LJ,fm})}{F_{LJ}(R_{LJ,a2}) - F_{LJ}(R_{LJ,fm})}. \tag{34}$$

From the results in the first part of this paper and in ref 33, a conservative choice for R_{a2} is one for which $|F'(R_{a2})| > (F_{fm}/2.0)$.

Proceeding inductively, by choosing additional R-values for the target force curve and calculates the associated R-values for the reference force curve according to eq 32 and then constructs approximations to $F(R)$ on $R_{aj} < R < R_{aj+1}$ in a manner analogous to eqs 33 and 34. A conservative choice for R_{aj} would be one for which $|F'(R_{aj})| > (F_{fm}/2^j)$. For the examples given in Table 7, $j = 3$. A measure of how far along the tail of the force distribution to approximation goes is given by $|F(R_{a3})|/F_m$. This ratio for the four molecules H_2, H_2^+, Ar_2, and water dimer takes the values 0.041, 0.082, 0.035 and 0.077, respectively.

V. Conclusions

In the first part of this work, adaption of previously developed canonical approaches for application to algebraic forms of the classic Morse, Lennard-Jones, and Kratzer potentials have been developed. Using the canonical transformation generated for the Morse potential as a reference, inverse transformations are generated for potentials including the H_2^+ ion, neutral covalently bound H_2, van der Waals bound Ar_2, and the hydrogen bonded one dimensional dissociative coordinate in water dimer. Similar constructions have also been developed for Lennard-Jones and Kratzer potentials. The methodology developed in this work can also be applied to any of the 100 plus currently available algebraic potential functions.[7] A benefit of this canonical approach, in contrast to classical approaches, to the application of these algebraic potential functions has been demonstrated by significantly improved generation of eigenvalues for the potentials in the pairwise interactions studied. In particular, these classical algebraic functions involve a number of adjustable parameters and in general they do not accurately represent the potential curve of a real molecule as they have been traditionally utilized. In the present canonical approach to algebraic potentials functions, the adjustable parameters are of

limited significance but more accurate representations of the potential curve of a real molecule are obtained.

The second part of this work presents an algorithmic strategy based upon a canonical transformation to dimensionless form applied to the force distribution associated to a potential. In addition to leading to accurate approximations to both the force and potential functions corresponding to a particular diatomic molecule in terms of the force distribution associated to an algebraic potential function, such as the Lennard-Jones function, this canonical force approach also provides a means to deriving accurate approximations to the dissociation energy D_e, the equilibrium nuclear separation distance R_e, the maximum attractive force F_m, and the internuclear separation R_{am} at which the maximum force obtains.

References

(1) Kaplan, I. G. *Intermolecular Interactions: Physical Picture, Computational Methods and Model Potentials*; Wiley: England, 2006.

(2) Stone, A. J. *The Theory of Intermolecular Forces*, 2nd ed.; Oxford University Press: Oxford, U.K., 2013.

(3) Csaśzaŕ, A. G.; Allen, W. D.; Yamaguchi, Y.; Schaefer III, H.F. Ab Initio Determination of

Accurate Ground Electronic State Potential Energy Hypersurfaces for Small Molecules. In *Computational Molecular Spectroscopy*; Jensen, P., Bunker, P. R., Eds.; Wiley: New York, 2000; pp. 15-68.

(4) Tang, K. T.; Toennies, J. P. An Improved Simple Model for the van der Waals Potential Based on Universal Damping Functions for the Dispersion Coefficients. *J. Chem. Phys.* **1984**, *80*, 3726-3741.

(5) Hajigeorgiou, P. G.; Le Roy, R. J. A "Modified Lennard-Jones Oscillator" Model for Diatom Potential Functions. *J. Chem. Phys*. **2000**, *112*, 3949-3957.

(6) Cahill, K.; Parsegian, V. A. Rydberg−London Potential for Diatomic Molecules and Unbonded Atom Pairs. *J. Chem. Phys*. **2004**, *121*, 10839-10842.

(7) Xie, J. C.; Mishra, S. K.; Kar, T.; Xie, R.-H. Generalized Interatomic Pair-Potential Function. *Chem. Phys. Lett.* **2014**, *605-606*, 137-146.

(8) Ibarra-Tandi, B.; Lira, A.; López-Lemus, J. Effect of Softness on Relative Adsorption for Binary Mixtures of Simple Fluids. *J. Mol. Liq.* **2013**, *185*, 62-69.

(9) Xie, R.-H.; Hsu, P. S. Universal Reduced Potential Function for Diatomic Systems. *Phys. Rev. Lett.* **2006**, *96*, 243201.

(10) Tellinghuisen, J.; Henderson, S. D.; Austin, D.; Lawley, K. P.; Donovan, R. J. Reduced Potential-Energy Curves for Diatomic Molecules. *Phys. Rev. A* **1989**, *39*, 925-930.

(11) Lim, T.-C. Relationship and Discrepancies Among Typical Interaction Potential Functions. *Chin. Phys. Lett*. **2004**, *21*, 2167-2170.

(12) Lim, T.-C. Connection Among Classical Interatomic Potential Functions. *J. Math. Chem*. **2004**, *36*, 261-269.

(13) LeSar, L. *Introduction to Computational Materials Science*; Cambridge University Press: Cambridge, 2013; pp. 62-92.

(14) Martinez, J. A.; Yilmaz, D. E.; Liang, T.; Sinnott, S. B.; Phillpott, S. R. Fitting Empirical Potentials: Challenges and Methodologies. *Curr. Opin. Solid State Mater. Sci.* **2013**, *17*, 263-270.

(15) Mackerell, Jr., A. D. Empirical Force Fields for Biological Macromolecules: Overview and Issues. *J. Comput. Chem*. **2004**, *25*, 1584-1604.

(16) Harding, J. H. Interionic Potentials: A User Guide. In *Computer Simulation in Materials Science*, Meyer, M.; Pontikis, V. Eds; Kluwer Academic Publishers: Dordrecht, 1991.

(17) Song, Y.; Tyka, M.; Leaver-Fay, A.; Thompson, J.; Baker, D. Structure-Guided Forcefield Optimization. *Proteins* **2011**, *79*, 1898-1909.

(18) Jones, J. E. On the Determination of Molecular Fields. II. From the Equation of State of a Gas. *Proc. R. Soc. Lond. A* **1924**, *106*, 463-477.

(19) Hajigeorgiou, P. G. An Extended Lennard-Jones Potential Energy Function for Diatomic Molecules: Application to Ground Electronic States. *J. Mol. Spectrosc*. **2010**, *263*, 101-110.

(20) Mie, G. Zur Kinetischen Theorie der Einatomigen Körper. *Ann. Phys*. **1903**, *316*, 657-697.

(21) Kratzer, A. Die Ultraroten Rotationsspektren der Halogenwasserstoffe. *Z. Phys*. **1920**, *3*, 289-307.

(22) Van Hooydonk, G. A Universal Two-Parameter Kratzer-Potential and Its Superiority Over Morse's for Calculating and Scaling First-Order Spectroscopic Constants of 300 Diatomic Bonds. *Eur. J. Inorg. Chem*. **1999**, *1999*, 1617-1642.

(23) Morse, P. M. Diatomic Molecules According to the Wave Mechanics. II. Vibrational Levels. *Phys. Rev*. **1929**, *34*, 57-64.

(24) Xantheas, S. S.; Werhahn, J. C. Universal Scaling of Potential Energy Functions Describing Intermolecular Interactions. I. Foundations and Scalable Forms of New Generalized Mie, Lennard-Jones, Morse, and Buckingham Exponential-6 Potentials. *J. Chem. Phys*. **2014**, *141*, 064117.

(25) Plíva, J. A Closed Rovibrational Energy Formula Based on a Modified Kratzer Potential. *J. Mol. Spectrosc*. **1999**, *193*, 7-14.

(26) Han, D.; Song, X.-H.; Yang, X. Study for Diatomic Molecule by Supersymmetric Quantum Mechanics Approach and an Identified Method to Morse Potential. *Physica A* **2005**, *345*, 485-492.

(27) Cheng, L.; Yang, J. Modified Morse Potential for Unification of the Pair Interactions. *J. Chem. Phys*. **2007**, *127*, 124104.

(28) Sesma, J. Exact Solution of the Schrödinger Equation with a Lennard-Jones Potential. *J. Math. Chem*. **2013**, *51*, 1881-1896.

(29) Setare, M. R.; Karimi, E. Algebraic Approach to the Kratzer Potential. *Phys. Scr*. **2007**, *75*, 90-93.

(30) Lucchese, R. R.; Rosales, C. K.; Rivera-Rivera, L. A.; McElmurry, B. A.; Bevan, J. W.; Walton, J. R. A Unified Perspective on the Nature of Bonding in Pairwise Interatomic Interactions. *J. Phys. Chem. A* **2014**, *118*, 6287-6298. In this reference, the notation $V(R)$ corresponds to the notation $E(R)$ used in the current work.

(31) Walton, J. R.; Rivera-Rivera, L. A.; Lucchese, R. R.; Bevan, J. W. A General Transformation to Canonical Form for Potentials in Pairwise Interatomic Interactions. *Phys. Chem. Chem. Phys*. **2015**, *17*, 14805-14810.

(32) Walton, J. R.; Rivera-Rivera, L. A.; Lucchese, R. R.; Bevan, J. W. A Canonical Approach to Forces in Molecules. *Chem. Phys.* **2016**, *474*, 52-58.

(33) Walton, J. R.; Rivera-Rivera, L. A.; Lucchese, R. R.; Bevan, J. W. Canonical Potentials and Spectra within the Born–Oppenheimer Approximation. *J. Phys. Chem. A* **2015**, *119*, 6753-6758. In this reference, the notation $V(R)$ corresponds to the notation $E(R)$ used in the current work.

(34) Feynman, R. P. Forces in Molecules. *Phys. Rev.* **1939**, *56*, 340-343.

(35) Pachucki, K. Born-Oppenheimer Potential for H_2. *Phys. Rev. A* **2010**, *82*, 032509.

(36) Private communication from Schwenke, D. W., who supplied the H_2^+ data.

(37) Jäger, B.; Hellmann, R.; Bich, E.; Vogel, E. Ab Initio Pair Potential Energy Curve for the Argon Atom Pair and Thermophysical Properties of the Dilute Argon Gas. I. Argon-Argon Interatomic Potential and Rovibrational Spectra. *Mol. Phys.* **2009**, *107*, 2181-2188.

(38) Shank, A.; Wang, Y.; Kaledin, A.; Braams, B. J.; Bowman, J. M. Accurate Ab Initio and "Hybrid" Potential Energy Surfaces, Intramolecular Vibrational Energies, and Classical IR Spectrum of the Water Dimer. *J. Chem. Phys.* **2009**, *130*, 144314.

(39) Cooley, J. W. An Improved Eigenvalue Corrector Formula for Solving the Schrödinger Equation for Central Fields. *Math. Comput.* **1961**, *15*, 363-374.

(40) Brooks, B. R.; Bruccoleri, R. E.; Olafson, B. D.; States, D. J.; Swaminathan, S.; Karplus, M. CHARMM: A Program for Macromolecular Energy, Minimization, and Dynamics Calculations. *J. Comput. Chem.* **1983**, *4*, 187-217.

(41) Cornell, W. D.; Cieplak, P.; Bayly, C. I.; Gould, I. R. Merz, K. M.; Ferguson, D. M.; Spellmeyer, D. C.; Fox, T.; Caldwell, J. W.; Kollman, P. A. A Second Generation Force Field for the Simulation of Proteins, Nucleic Acids, and Organic Molecules. *J. Am. Chem. Soc.* **1995**, *117*, 5179-5197.

(42) Lifson, S.; Hagler, A. T.; Dauber, P. Consistent Force Field Studies of Intermolecular Forces in Hydrogen-Bonded Crystals. 1. Carboxylic Acids, Amides, and the C=O-H- Hydrogen Bonds. *J. Am. Chem. Soc.* **1979**, *101*, 5111-5121.

(43) Rappe, A. K.; Casewit, C. J.; Colwell, K. S.; Goddard III, W. A.; Skiff, W. M. UFF, a Full Periodic Table Force Field for Molecular Mechanics and Molecular Dynamics Simulations. *J. Am. Chem. Soc.* **1992**, *114*, 10024-10035.

(44) Walton, J. R.; Rivera-Rivera, L. A.; Lucchese, R. R.; Bevan, J. W. Canonical Approaches to Applications of the Virial Theorem. *J. Phys. Chem. A* **2016**, *120*, 817-823.

Table 1. Relative error between $E(R)$ and $\tilde{E}(R)$.[a]

	Relative Error		Relative Error		Relative Error		Relative Error
H_2^+-M	0.00173	H_2-M	0.00203	Ar_2-M	0.000475	WD-M	0.00131
H_2^+-LJ	0.00183	H_2-LJ	0.00227	Ar_2-LJ	0.000872	WD-LJ	0.000757
H_2^+-K	0.00186	H_2-K	0.00315	Ar_2-K	0.0037	WD-K	0.00271

[a] M: Morse; LJ: Lennard-Jones; K: Kratzer; WD: water dimer.

Table 2. Key internuclear separation distances required in eq 11.[a]

	R_{r5}	R_{r3}	R_{r1}	R_{rm}	R_e	R_{am}	R_{a1}	R_{a3}	R_{a5}
H_2^+	0.4115	0.6371	0.8507	0.9292	1.0568	1.5967	2.6161	3.7127	4.6464
H_2^+-M	0.1100	0.5169	0.8139	0.9102	1.0568	1.5967	2.5532	3.7307	4.8299
H_2^+-LJ	0.8803	0.9525	1.0086	1.0275	1.0568	1.1717	1.4039	1.7486	2.1424
H_2^+-K	0.5062	0.6972	0.8776	0.9449	1.0568	1.5853	3.1705	7.1711	14.9741
H_2	0.2751	0.4333	0.5898	0.6475	0.7414	1.131	1.788	2.3969	2.8934
H_2-M	0.0582	0.3519	0.5661	0.6356	0.7414	1.131	1.8211	2.6708	3.4639
H_2-LJ	0.6175	0.6682	0.7076	0.7208	0.7414	0.822	0.9848	1.2268	1.503
H_2-K	0.3551	0.4891	0.6156	0.6629	0.7414	1.1121	2.2243	5.0308	10.5051
Ar_2	3.0729	3.3706	3.5859	3.6557	3.7617	4.155	4.8822	5.9103	7.1038
Ar_2-M	3.072	3.3684	3.5847	3.6549	3.7617	4.155	4.8517	5.7095	6.5102
Ar_2-LJ	3.1332	3.3902	3.5901	3.6573	3.7617	4.1705	4.9969	6.2241	7.6258
Ar_2-K	1.8018	2.4816	3.1236	3.3634	3.7617	5.6426	11.2851	25.5247	53.2988
WD	2.2161	2.5116	2.7372	2.8117	2.9264	3.3648	4.2065	5.4354	7.4378
WD-M	2.1576	2.488	2.7291	2.8074	2.9264	3.3648	4.1415	5.0977	5.9902
WD-LJ	2.4375	2.6374	2.7929	2.8452	2.9264	3.2445	3.8874	4.842	5.9325
WD-K	1.4017	1.9306	2.43	2.6165	2.9264	4.3896	8.7793	19.8569	41.4639

[a] All values are in Å. M: Morse; LJ: Lennard-Jones; K: Kratzer; WD: water dimer.

Table 3. Vibrational Eigenvalues for H_2.

v	E_v (cm^{-1}) Accurate	E_v (cm^{-1}) Canonical	E_v (cm^{-1}) Morse
0	-36112.63	-36130.26	-36305.10
1	-31949.29	-31983.79	-32488.22
2	-28021.56	-28046.65	-28883.28
3	-24324.59	-24332.32	-25490.27
4	-20855.34	-20845.27	-22309.20
5	-17612.84	-17591.55	-19340.07
6	-14598.42	-14575.24	-16582.87
7	-11816.09	-11798.53	-14037.60
8	-9273.10	-9262.63	-11704.28
9	-6980.74	-6970.86	-9582.88
10	-4955.40	-4940.43	-7673.43
11	-3220.16	-3209.66	-5975.91
12	-1807.04	-1803.32	-4490.32
13	-760.45	-757.19	-3216.67
14	-141.80	-141.09	-2154.96
15			-1305.20
16			-667.95
17			-249.92
18			-39.32

Table 4. Vibrational Eigenvalues for H_2^+.

v	E_v (cm^{-1}) Accurate	E_v (cm^{-1}) Canonical	E_v (cm^{-1}) Morse
0	-21375.95	-21387.60	-21424.69
1	-19183.93	-19207.10	-19305.42
2	-17119.24	-17136.83	-17296.50
3	-15177.66	-15186.92	-15397.93
4	-13355.62	-13360.06	-13609.69
5	-11650.20	-11650.66	-11931.80
6	-10059.10	-10057.15	-10364.26
7	-8580.67	-8578.11	-8907.06
8	-7213.92	-7212.25	-7560.20
9	-5958.50	-5957.66	-6323.69
10	-4814.81	-4813.33	-5197.52
11	-3784.00	-3780.30	-4181.70
12	-2868.09	-2864.38	-3276.22
13	-2069.99	-2068.40	-2481.09
14	-1393.73	-1393.92	-1796.29
15	-844.47	-844.37	-1221.85
16	-428.69	-428.65	-757.74
17	-153.72	-153.83	-404.01
18	-23.86	-24.59	-161.69
19			-35.79

Table 5. Vibrational Eigenvalues for Ar_2 and water dimer.

v	E_v (cm^{-1}) Accurate	E_v (cm^{-1}) Canonical	E_v (cm^{-1}) Morse
		Ar_2	
0	-84.63	-84.64	-83.98
1	-58.93	-58.95	-56.93
2	-38.42	-38.44	-35.12
3	-22.90	-22.92	-18.55
4	-12.01	-12.04	-7.23
5	-5.19	-5.21	-1.14
6	-1.60	-1.60	
		Water Dimer	
0	-1657.91	-1658.16	-1652.67
1	-1497.73	-1498.22	-1481.46
2	-1347.38	-1347.75	-1319.62
3	-1206.68	-1207.03	-1167.13
4	-1075.46	-1075.96	-1024.01
5	-953.54	-954.04	-890.24
6	-840.74	-841.17	-765.83
7	-736.88	-737.16	-650.78
8	-641.75	-641.96	-545.09
9	-555.18	-555.48	-448.76
10	-476.94	-477.68	-361.79
11	-406.79	-407.95	-284.17
12	-344.45	-345.58	-215.92
13	-289.58	-290.46	-157.03
14	-241.74	-242.26	-107.49
15	-200.40	-200.76	-67.31
16	-164.90	-165.53	-36.50
17	-134.50	-135.30	-15.04
18	-108.46	-108.99	-2.94
19	-86.09	-86.29	
20	-66.83	-66.81	
21	-50.25	-50.23	
22	-36.03	-36.09	
23	-23.96	-23.98	
24	-13.87	-13.92	
25	-5.69	-5.73	

Table 6. Approximations of D_e, R_e, R_{am}, and F_m using the Lennard-Jones canonical transformation.[a]

	H_2	H_2^+	Water Dimer	Ar_2
R_0/Å	0.8	1.07	3.0	3.8
R_1/Å	1.0	1.65	3.2	4.0
R_2/Å	1.1	1.3	3.3	4.2
R_3/Å	1.2	1.65	3.5	4.25
R_4/Å	1.5	2.0	3.7	4.4
D_e/cm^{-1}	38304.9 (38293.0)	22528.6 (22525.7)	1741.67 (1741.78)	99.474 (99.465)
R_e/Å	07497 (0.741)	1.0564 (1.0568)	2.927 (2.964)	3.763 (3.762)
R_{am}/Å	1.131 (1.131)	1.588 (1.597)	3.368 (3.365)	4.159 (4.155)
F_m/(cm^{-1}/Å)	37485.3 (37488.6)	14220.5 (14196.6)	1187.74 (1186.9)	80.147 (80.254)
R_{fm}/Å	1.616 (1.606)	2.22 (2.223)	3.7996 (3.806)	4.547 (4.537)
F_{fm}/(cm^{-1}/Å)	36085.59 (36066.1)	8513.65 (8514.46)	858.51 (861.33)	67.97 (67.94)

[a] The numbers in parentheses are the accurate values of the indicated parameters. The indicated values for R_0, R_1, and R_2 are those chosen for use in solving the algebraic systems in eqs 16 and 20, and R_3, and R_4 are those chosen for use in solving the algebraic systems in eq 27.

Table 7. Approximation of $F(R)$ using the Lennard-Jones canonical transformation and the associated approximation of $E(R)$ by integration of the $F(R)$ approximation.[a]

	H_2	H_2^+	Water Dimer	Ar_2
R_{r4}/Å	0.4 (0.659)	0.55 (0.927)	2.0 (2.285)	3.0 (3.074)
R_{r3}/Å	0.48 (0.681)	0.65 (0.956)	2.2 (2.427)	3.15 (3.198)
R_{r2}/Å	0.52 (0.691)	0.75 (0.983)	2.4 (2.562)	3.35 (3.422)
R_{r1}/Å	0.58 (0.705)	0.88 (1.0157)	2.6 (2.698)	3.55 (3.556)
R_{rm}/Å	0.65 (0.721)	0.95 (1.0324)	2.8 (2.837)	3.65 (3.652)
R_{a2}/Å	2.2 (1.0528)	3.0 (1.446)	4.8 (4.336)	5.5 (5.698)
R_{a3}/Å	2.8 (1.294)	4.0 (1.724)	6.0 (5.393)	7.0 (7.518)
$F(R)$ Relative Error	0.00256 (0.00421)	0.00192 (0.00447)	0.00131 (0.00408)	0.00173 (0.00346)
$E(R)$ Relative Error	0.00473 (0.00156)	0.00272 (0.00224)	0.000573 (0.00224)	0.00292 (0.00496)

[a] The R-values in parentheses are the corresponding values for the reference Lennard-Jones force curve. The $F(R)$ and $E(R)$ relative errors in parentheses are for the repulsive-side of the curves $R < R_e$ while the values not in parentheses are for the attractive-side $R_e < R$.
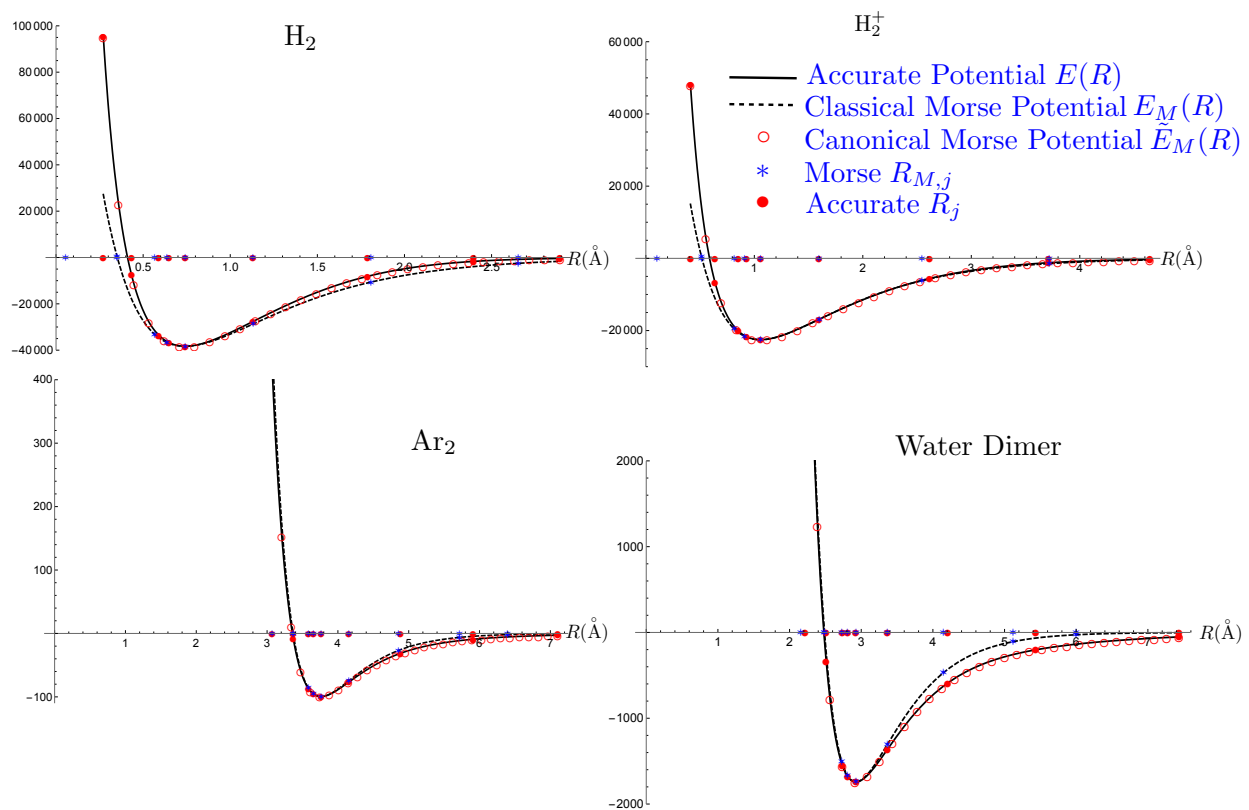
Morse Canonical Approximations

Figure 1. Graphs of $E(R)$, $E_M(R)$ and $\tilde{E}_M(R)$ for H_2, H_2^+, Ar_2 and the water dimer complex. The units of the ordinate are in cm^{-1}.
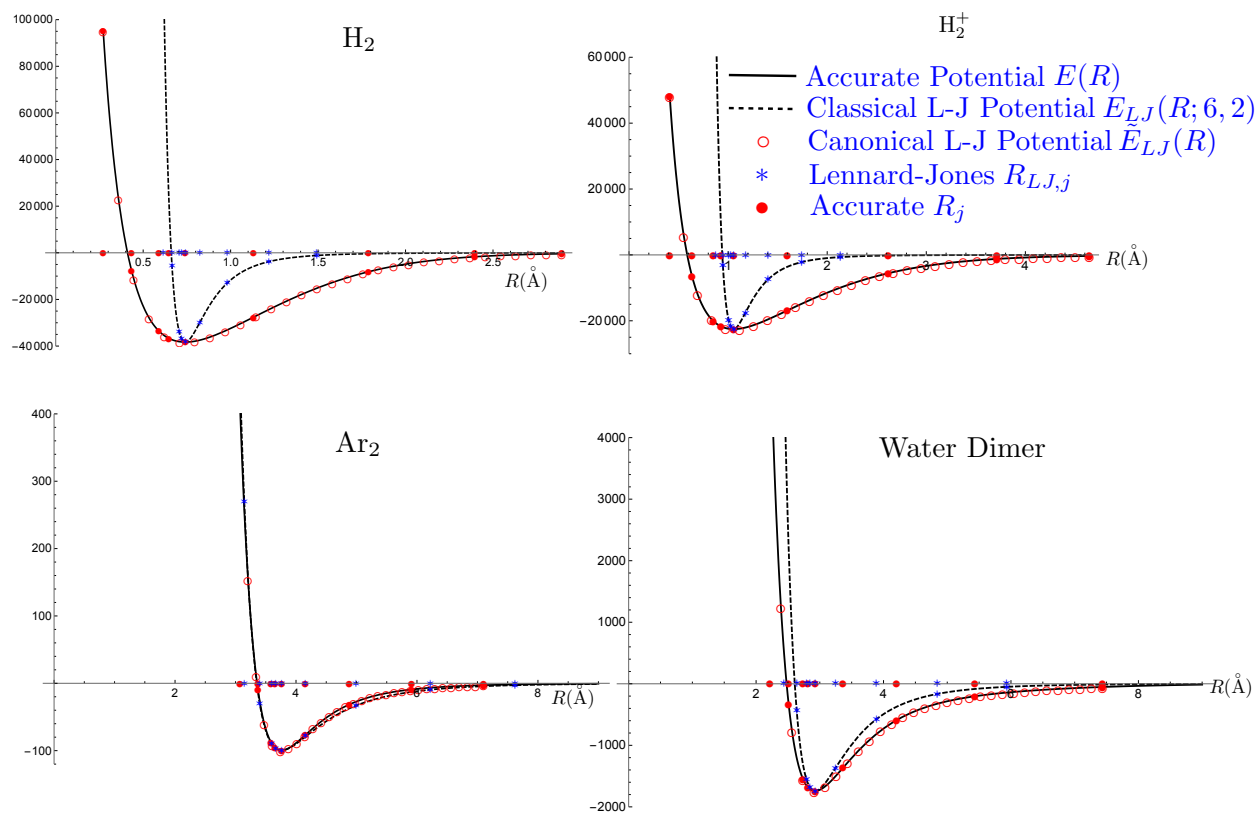
Lennard-Jones Canonical Approximations

Figure 2. Graphs of $E(R)$, $E_{\mathrm{LJ}}(R)$ and $\tilde{E}_{\mathrm{LJ}}(R)$ for H_2, H_2^+, Ar_2 and the water dimer complex. The units of the ordinate are in cm^{-1}.
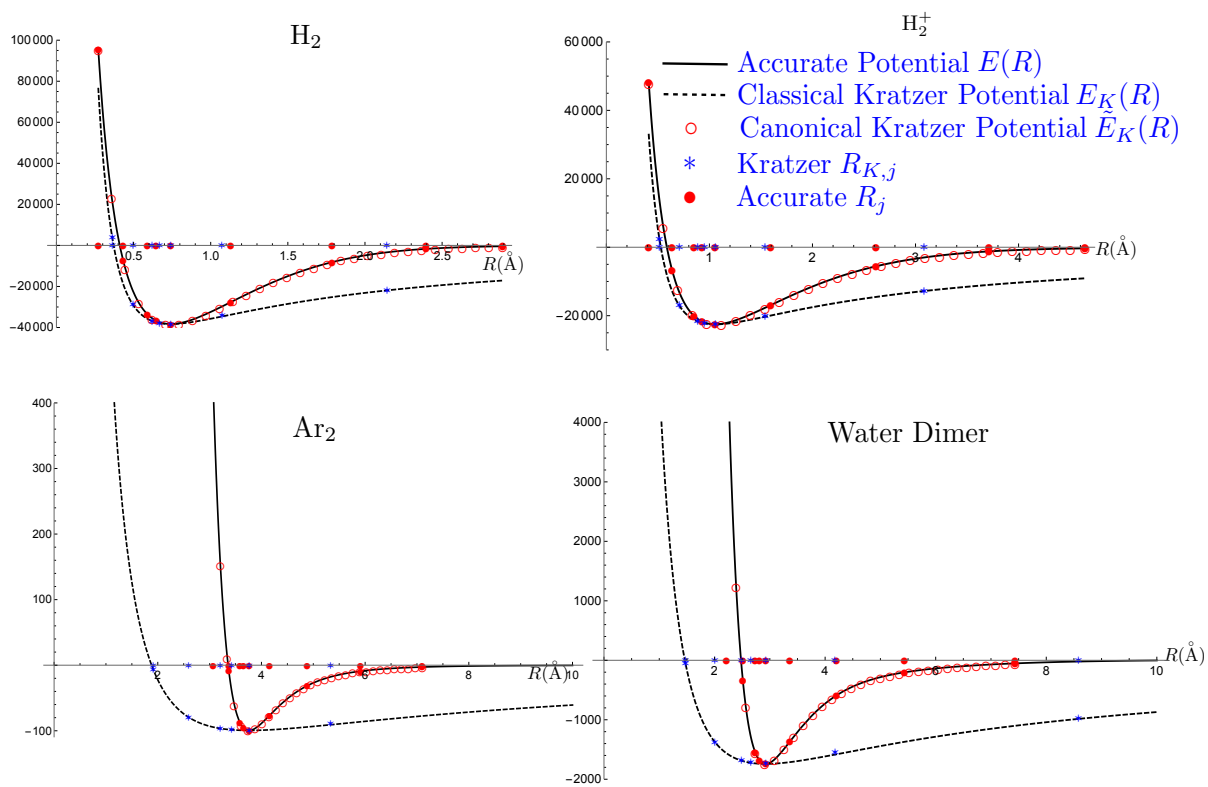
Kratzer Canonical Approximations

Figure 3. Graphs of $E(R)$, $E_K(R)$ and $\tilde{E}_K(R)$ for H$_2$, H$_2^+$, Ar$_2$ and the water dimer complex. The units of the ordinate are in cm^{-1}.

Table of Contents Graphic

H_2^+

— Accurate Potential $E(R)$
---- Classical L-J Potential $E_{LJ}(R; 6, 2)$
○ Canonical L-J Potential $\tilde{E}_{LJ}(R)$
✳ Lennard-Jones $R_{LJ,j}$
● Accurate R_j

$R(\overset{\circ}{A})$